NIH Public Access
Author Manuscript
Dev Biol. Author manuscript; available in PMC 2012 April 26.

Published in final edited form as:
Dev Biol. 2007 October 1; 310(1): 140–153. doi:10.1016/j.ydbio.2007.07.038.

TGF-β mediated *Msx2* expression controls occipital somites-derived caudal region of skull development

Ryoichi Hosokawa[1], **Mark Urata**[1], **Jun Han**[1], **Armen Zehnaly**[1], **Pablo Bringas Jr.**[1], **Kazuaki Nonaka**[2], and **Yang Chai**[1,*]

[1]Center for Craniofacial Molecular Biology, University of Southern California, Los Angeles, CA 90033

[2]Division of Oral Health, Growth & Development, Kyushu University, School of Dentistry, Kyushu, Japan

Abstract

Craniofacial development involves cranial neural crest (CNC) and mesoderm-derived cells. TGF-β signaling plays a critical role in instructing CNC cells to form the craniofacial skeleton. However, it is not known how TGF-β signaling regulates the fate of mesoderm-derived cells during craniofacial development. In this study, we show that occipital somites contribute to the caudal region of mammalian skull development. Conditional inactivation of *Tgfbr2* in mesoderm-derived cells results in defects of the supraoccipital bone with meningoencephalocele and discontinuity of the neural arch of the C1 vertebra. At the cellular level, loss of TGF-β signaling causes decreased chondrocyte proliferation and premature differentiation of cartilage to bone. Expression of *Msx2*, a critical factor in the formation of the dorsoventral axis, is diminished in the *Tgfbr2* mutant. Significantly, overexpression of *Msx2* in *Myf5-Cre;Tgfbr2*$^{flox/flox}$ mice partially rescues supraoccipital bone development. These results suggest that the TGF-β/Msx2 signaling cascade is critical for development of the caudal region of the skull.

Keywords

Occipital somite; cell proliferation; differentiation; occipital bone development; cervical vertebrae; Myf5; TGF-β; Msx2; mouse

Introduction

Craniofacial development involves two distinct mesenchymal cell lineages, mesoderm-derived cells and cranial neural crest cells (ectomesenchymal cells), both of which give rise to skeletal and mesenchymal tissues (Morriss-Kay, 2001; Noden and Trainor, 2005). Craniofacial bone is divided into two components, the neurocranium and the viscerocranium. The neurocranium forms the braincase and is constructed from both mesodermal- and neural crest-derived structures. The viscerocranium develops from the

© 2007 Elsevier Inc. All rights reserved.

*Author for correspondence: Dr. Yang Chai, Center for Craniofacial Molecular Biology, University of Southern California, 2250 Alcazar Street, CSA 103, Los Angeles, California 90033, Tel. (323)442-3480, Fax (323)442-2981, ychai@usc.edu.

Publisher's Disclaimer: This is a PDF file of an unedited manuscript that has been accepted for publication. As a service to our customers we are providing this early version of the manuscript. The manuscript will undergo copyediting, typesetting, and review of the resulting proof before it is published in its final citable form. Please note that during the production process errors may be discovered which could affect the content, and all legal disclaimers that apply to the journal pertain.

NIH-PA Author Manuscript
NIH-PA Author Manuscript
NIH-PA Author Manuscript

NIH-PA Author Manuscript

NIH-PA Author Manuscript

NIH-PA Author Manuscript

pharyngeal arch complex, forms the anterior part of the face, and is composed entirely of neural crest-derived structures (Kuratani, 2005).

Recently, transgenic mouse models have revealed the significance of TGF-β signaling in regulating craniofacial development. *Tgfb2* null mice show defects in the supraoccipital and alisphenoid bones and the pterygoid process. These mice also have small mandibles and lack coronoid and condyle processes, which are neural crest-derived elements (Sanford et al., 1997). *Tgfb2*$^{-/-}$;*Tgfb3*$^{-/-}$ mice also show skull defects in both mesoderm- and neural crest-derived structures (Dunker and Krieglstein, 2002). The conventional knockout model of Smad2, one of the intercellular mediators of TGF-β signaling, shows compromised facial axis formation during embryonic development (Heyer et al., 1999). Some haplosufficient *Smad2* mice show loss of the mandible and eye (Nomura and Li, 1998, our unpublished data). Taken together, these findings imply that TGF-β signaling is critical for patterning both neural crest cells and mesoderm-derived cells during craniofacial development.

Multiple TGF-β isoforms induce a TGF-β signaling response through type I and type II receptors. Previous study has shown that *Tgfbr2* null mutant mice die prematurely at day E11.5, and chimeric mice show agnathia with anophthalmia and hydrocephalus with internal hemorrhage (Oshima et al., 1996). To overcome the early embryonic lethal phenotype, we generated *Tgfbr2* conditional knockout mice using Cre-Loxp recombinant technology in order to explore tissue specific requirements for TGF-β signaling during embryonic development. We have already reported that TGF-β signaling plays a critical role in regulating neural crest cells during the development of craniofacial structures (Ito et al., 2003; Sasaki et al., 2006). In particular, *Wnt1-Cre;Tgfbr2*$^{flox/flox}$ mice show a frontal bone (neurocranium) defect and small mandible (viscerocranium). In the present report, we investigate the function of TGF-β signaling in mesoderm-derived cells during occipital bone development.

Myf5 is a member of the Myogenic Regulatory Factors (MRFs) family and is implicated in the process of skeletal muscle development (Braun et al., 1992; Weintraub et al., 1991). *Myf5* transcripts are first detected on embryonic day E8.0 in cells of the dorsal medial quadrant of the somite in the prospective epaxial domain (Ott et al., 1991; Tajbakhsh et al., 1996). *Myf5* expression is also detected at day E8.0 in the occipital mesoderm, which gives rise to bone and muscle components around the occipital area (Huang et al., 2000; Ott et al., 1991). Furthermore, *Myf5* null mice exhibit defects in somite and rib formation, but not in muscle formation (Braun et al., 1992; Grass et al., 1996). Clearly, *Myf5* is expressed broadly in mesoderm-derived cells, not limited to skeletal muscle precursors. These characteristics suggest that *Myf5-Cre* mice, when crossed with *Tgfbr2* floxed mice, are a suitable model for the investigation of the function of TGF-β signaling in regulating mesoderm-derived cells during embryonic development (Tallquist et al., 2000).

Myf5-Cre;Tgfbr2$^{flox/flox}$ mice survive until birth and show defective supraoccipital bone development with meningoencephalocele, discontinuity of the neural arch of the C1 vertebra, and accelerated differentiation of chondrocytes. Expression of *Msx2*, a critical factor for dorsovental axis formation (Takahashi and Le Douarin, 1990; Takahashi et al., 1992), is diminished in the mid-dorsal area at day E10.5. Moreover, transgenic mice overexpressing *Msx2* exhibit a partial rescue of the supraoccipital bone defect in *Tgfbr2* mutant mice. Our findings suggest that the TGF-β/Msx2 signaling cascade plays an important role in regulating the development of the occipital somite-derived caudal region of the skull.

NIH-PA Author Manuscript
NIH-PA Author Manuscript
NIH-PA Author Manuscript

Materials and Methods

Generation of *Myf5-Cre;Tgfbr2$^{flox/flox}$* and *Myf5-Cre;Tgfbr2$^{flox/flox}$;Msx2$^{TG/+}$* mice

All animal studies were performed according to IACUC guidelines. *Myf5-Cre* transgenic mice have been described previously (Tallquist et al., 2000). We crossed *Myf5-Cre;Tgfbr2$^{flox/+}$* with *Tgfbr2$^{flox/flox}$* mice to generate *Myf5-Cre;Tgfbr2$^{flox/flox}$* null alleles that were genotyped using PCR primers as previously described (Chytil et al., 2002).

Myf5-Cre;Tgfbr2$^{flox/flox}$;Msx2$^{TG/+}$ mice were described previously (Liu et al., 1999). To confirm the overexpression of *Msx2* gene, PCR was performed using standard methods (Hosokawa et al., 2005). mRNA was extracted from the dorsal side of somites at E10.5 following standard methods.

Two-component genetic system for marking the progeny of somite-derived cells

The *R26R* conditional reporter allele has been described previously (Soriano, 1999). We mated *Myf5-Cre* and *R26R* mice to generate *Myf5-Cre;R26R* embryos. Detection of β-galactosidase activity in whole embryos (E9.5) was carried out as previously described (Chai et al., 2000).

Myf5-Cre/R26R reporter assay

Myf5-Cre;Tgfbr2$^{flox/+}$ mice were crossed with *Tgfbr2$^{foxl/flox}$;R26R$^{flox/flox}$* mice to produce embryos with the genotype of *Myf5-Cre;Tgfbr2$^{flox/flox}$;R26R$^{flox/+}$*. β-galactosidase analysis was carried out as described (Sasaki et al., 2006).

Staining of whole skeleton

Whole skeletal preparations of newborn mice were prepared and stained with Alizarin Red and Alcian Blue as previously described (McLeod, 1980).

Histological analysis

Tissues were fixed in 4 % paraformaldehyde in phosphate buffered saline, decalcified in Decalcifying solution (Richard-Allan Scientific, Kalamazoo, MI), paraffin embedded, sectioned at 7 μm and stained with hematoxylin/eosin and Safranin O/Fast Green. For immunostaining, tissue sections were incubated with anti-Myf5 (1:500, Santa Cruz biotechnology Inc, Santa Cruz, CA), anti-TGF-β IIR (1:100, Santa Cruz biotechnology Inc, Santa Cruz, CA) and anti-CD45 antibody (1:50, Santa Cruz biotechnology Inc, Santa Cruz, CA) using standard procedures. For Safranin O/Fast Green staining, deparaffined and rehydrated sections were stained in hematoxylin (Sigma, St. Louis, MO), 0.001% Fast Green (Sigma) followed by a rinse in 1 % acetic acid and 0.1 % Safranin O (Sigma) (Stickens et al., 2004).

BrdU labeling/histology

A 10 mg/ml stock of bromodeoxyuridine (BrdU; Sigma, St Louis, MO) was injected intraperitoneally into mice at E13.5 and E14.5 at a dose of 100 μg BrdU per gram of body weight. Mice were sacrificed 1 hour after injection and embryos were harvested. BrdU staining was carried out on paraffin sections by using a BrdU staining kit according to manufacturer's directions (Zymed, South San Francisco, CA).

In situ hybridization

Whole-mount and sectioned in situ hybridization were performed according to standard procedure (Wilkinson, 1998). Several negative controls (sense probe and no probe) were run in parallel with the experimental reaction. RNA probes were generated as reported

NIH-PA Author Manuscript

NIH-PA Author Manuscript

NIH-PA Author Manuscript

previously: *Type I collagen* (Sasaki et al., 2006), *Msx1* (Ishii et al., 2005), *Msx2* (Ishii et al., 2003), and *Shh* (Hui and Joyner, 1993).

Organ culture of wild type and *Myf5-Cre;Tgfbr2*$^{flox/flox}$ mutant mid-dorsal element explants

Timed-pregnant mice were sacrificed on postcoital day 10.5 and staged according to somite age. Mid-dorsal region including otic vesicle were cultured in serumless, chemically-defined BGJB medium according to standard methods (Chai et al., 1994).

Preparation and introduction of TGF-β beads

For delivery of TGF-β1 or TGF-β2, we used affi-gel blue beads (BioRad, Hercules, CA), diameter 50-80 μm. The beads were washed in phosphate-buffered saline (PBS) and then incubated for 1 hour at room temperature in 10 μg/ml TGF-β1 or TGF-β2 (R&D, Minneapolis, MN). Control beads were incubated in 0.1% BSA. TGF-β or BSA-containing beads were placed the same distance from the midline on the dorsal area of the explant. In wild-type and *Tgfbr2*$^{flox/flox}$*;Myf5-Cre* mutant samples, one side of the mid-dorsal region was treated with BSA beads and the other side treated with TGF-β beads.

Results

Myf5 promoter-driven LacZ positive cells populate mesoderm-derived structures

In order to investigate Cre recombination under the control of the *Myf5* promoter, we generated *Myf5-Cre;R26R*$^{flox/+}$ mice. Whole mount lacZ staining revealed that somites were positive (Fig. 1A). We stained sections to analyze the pattern and time course of the Cre recombination driven by the *Myf5* promoter (Figs. 1B-F). Somite-derived cells were lacZ positive (Fig. 1B). Furthermore, E13.5 *Myf5-Cre;R26R*$^{flox/+}$ embryos displayed unexpected LacZ positive cells in skeletal elements (Figs. 1C, D). LacZ positive cells were present not only in musculature primordia but also in the primordia of the supraoccipital bone, the neural arch of C1 vertebra, and the perichondrium of these primordia (Figs. 1C, D). At later developmental stages, a pattern of the lacZ craniofacial staining emerged based on cell origin. Supraoccipital bone, a somite-derived structure, possessed lacZ positive cells (Fig. 1E). On the other hand, the parietal bone, which is paraxial mesoderm-derived and not a somite-derived structure, was lacZ negative (Fig. 1F). To eliminate the possibility that osteoblasts and chondrocytes possess endogenous β-galactosidase activity, we checked the humerus, a lateral mesoderm-derived component. LacZ staining was seen only in myogenic cells (Fig. 1G, black arrow) but not the skeletal element (Fig. 1G, white arrow). In addition, we confirmed the localization of endogenous Myf5 expression in the supraoccipital bone primordium using immunohistochemistry. Myf5 positive nuclei were detectable in the primordium of the supraoccipital bone (Fig. 1H). Taken together, these results suggest that Cre recombination driven by the *Myf5* promoter will be produced only in somite-derived mesoderm cells that contributed to caudal skull development.

Myf5-Cre;Tgfbr2$^{flox/flox}$ mice show altered posture and hemorrhage around the occipital area at birth

After crossing *Tgfbr2*$^{flox/flox}$ and *Myf5-Cre;Tgfbr2*$^{flox/+}$ mice, we obtained 42 out of 127 pups that were *Myf5-Cre;Tgfbr2*$^{flox/flox}$. The ratio of newborn mice in the experimental group was slightly higher than the expected Mendelian ratio (33 % verse 25 %), suggesting that all conditional knockout mice could survive until birth. These *Tgfbr2* knockout mice showed a hunchback phenotype (Fig. 2A) and hemorrhage in the occipital area (Figs. 2A-C). Furthermore, the knockout produced meningoencephalocele in the occipital area and lethality at birth (Figs. 2D, E). To confirm that these defects were the result of *Tgfbr2* gene inactivation, we examined the expression of TGF-β IIR in the supraoccipital bone primordium. TGF-β IIR was expressed in the supraoccipital bone primordium (Fig. 2F,

NIH-PA Author Manuscript

NIH-PA Author Manuscript

NIH-PA Author Manuscript

black arrows) and the temporal bone primordium (Fig. 2F, white arrows) in the *Myf5-Cre;Tgfbr2*$^{flox/+}$ sample, whereas it was inactivated in the primordium of the supraoccipital bone in the *Myf5-Cre;Tgfbr2*$^{flox/flox}$ sample (Fig. 2G, black arrow). However, the primordium of the temporal bone, a LacZ negative area (see Fig. 1C), appeared to contain TGF-β IIR positive cells (Fig.2G, white arrows). These observations indicated the successful and specific inactivation of the *Tgfbr2* gene by Cre-mediated recombination.

Myf5-Cre;Tgfbr2$^{flox/flox}$ mice have defects in supraoccipital bone formation at the newborn stage

We used *Myf5-Cre;Tgfbr2*$^{flox/+}$ mice as control samples, and their development was indistinguishable from wild type. In control mice, the skull vault consists of the frontal, parietal, interparietal, and supraoccipital bones, from anterior to posterior (Figs. 3A, E). Although the frontal, parietal, and interparietal bones of conditional knockout mice developed normally, the supraoccipital bone was diminished at birth (Figs. 3B, F). There was only a small fragment of supraoccipital bone in the conditional knockout mice (Fig. 3J, black arrow), much smaller than that of control mice (Fig. 3I). In control mice, the foramen magnum, composed of the basioccipital, exoccipital, and supraoccipital bones, was conjugated with cartilage tissue (Fig. 3M). In conditional knockout mice, the foramen magnum was disconnected from the cartilage, most likely because of the diminished supraoccipital bone (Fig. 3N). Conditional knockout mice also showed disconnection of the C1 vertebra (Figs. 3Q, R).

Dorsal endochondral ossification defects in *Myf5-Cre;Tgfbr2*$^{flox/flox}$ mice

The skull vault has two ossification systems, intramembranous and endochondral (Noden, 1988). Quail-chicken chimera experiments have shown that the supraoccipital bone contains somite-derived cells and undergoes endochondral ossification (Couly et al., 1993; Huang et al., 2000). In the process of forming the supraoccipital bone and the neural arch of the vertebrae, the cartilage tissue expands into the middle of the dorsal region, and then each side of cartilage fuses. After that, endochondral ossification, the process the long bones of the trunk use for osteogenesis, begins in the supraoccipital bone and the neural arch of the vertebra (Figs. 4A, C, M, O). At birth, the control mice (*Myf5-Cre;Tgfbr2*$^{flox/+}$) showed continuous bone formation from lateral to dorsal (Fig. 4A, arrowheads), and the base of the supraoccipital bone contained chondrocytes (Fig. 4C). In contrast, conditional knockout mice (*Myf5-Cre;Tgfbr2*$^{flox/flox}$) showed hypoplasia of the supraoccipital bone such that the primordium could not expand towards the dorsal midline (Fig. 4B, black arrow) and part of the brain was outside the skull (Fig. 4B, white arrow). These hypoplastic supraoccipital bone primordia had already been transformed from cartilage to bone tissue (Fig. 4D). Each side of the neural arch of the C1 vertebra extended to the dorsal midline and then fused with the cartilage tissue in the control mouse (Figs. 4M, O). In contrast, each neural arch in the conditional knockout mice was disconnected in the dorsal region (Fig. 4N, asterisk). It appears that the edge of the neural arch contains only the hypertrophic zone (Fig. 4P). Safranin O staining clearly showed that conditional knockout mice lost the proliferating and resting zones in the supraoccipital bone and the neural arch of C1 vertebra at the newborn stage (Figs. 4E-H, Q-T). The supraoccipital bone of the conditional knockout mice instead contained a bone marrow-like structure (Fig. 4H, arrow), and the hypertrophic zone delineated the edge of the neural arch (Fig. 4T). Furthermore, we examined the expression of the *Type I collagen* gene, a marker for osteoblasts (Sasaki et al., 2006). In the control mice, only the bone adjacent to the hypertrophic zone contained *Type I collagen* positive cells (Fig. 4I). Strikingly, *Type I collagen* positive cells were detectable in the region of the hypotrophic as well as the hypertrophic zone in supraoccipital bone of *Myf5-Cre;Tgfbr2*$^{flox/flox}$ mice (Fig. 4J). To confirm the bone marrow structure, we performed immunostaining for CD45, a marker for hematopoietic cells (Yin and Li, 2006). We

NIH-PA Author Manuscript

NIH-PA Author Manuscript

NIH-PA Author Manuscript

detected CD45 positive cells within the bone structure (Figs. 4L) in the *Myf5-Cre;Tgfbr2*$^{flox/flox}$ mice, implying that bone marrow was contained within the bone. These observations suggest that the endochondral ossification process was compromised in the supraoccipital bone and C1 neural arch of *Myf5-Cre;Tgfbr2*$^{flox/flox}$ mice.

Compromised perichondrium formation and muscle attachment in *Myf5-Cre;Tgfbr2*$^{flox/flox}$ mice

In order to understand the cause of the endochondral ossification defects in *Myf5-Cre;Tgfbr2*$^{flox/flox}$ mice, we examined the early development of the supraoccipital bone and the neural arch of C1 at E15.5. Typically, the perichondrium of both the supraoccipital bone and the neural arch extends to the dorsal area (Figs. 5A, C, K, M). In control mice, the perichondrium was well formed (Fig. 5C, black arrow), and muscle tissue formed several layers and extended to the dorsal area (Fig. 5C, black arrowheads). In contrast, the expansion of muscle tissue was compromised in the conditional knockout mice (Fig. 5B, white arrowheads), and the perichondrium was disorganized at the tip of the cartilage (Fig. 5D, white arrow). The disorganized perichondrium was seen in the serial sections of supraoccipital bone primordium throughout the rostral to caudal regions (supplement figure). We also observed the disorganization of the perichondrium at the level of the neural arch of C1 vertebra (Figs. 5L, N, white arrow). Furthermore, muscle attachment to the primordium of the neural arch occurred early in conditional knockout mice (Fig. 5N, white arrowhead), beginning at E14.5 (data not shown). However, we did not observe any problems with organization at the lower level of cervical vertebra (data not shown). Interestingly, the differentiation of cartilage in the conditional knockout mice was indistinguishable from that of control mice at E15.5 (Figs. 5E-H, O-R). The primordia of the supraoccipital bone were composed of undifferentiated chondrocytes in both control and conditional knockout mice according to histological analysis (Figs. 5G, H). The primordia of the neural arch possessed three zones, hypertrophic, proliferating, and resting, in both control and conditional knockout mice (Figs. 5Q, R). Furthermore, we assessed *Type I collagen* expression to confirm whether osteogenic differentiation was accelerated. In control mice, the dorsal tip of the perichondrium was positive for *type I collagen* (Fig. 5I), implying that osteogenic precursors populated the area. In *Myf5-Cre;Tgfbr2*$^{flox/flox}$ mice, *type I collagen* expression was compromised in the dorsal tip (Fig. 5J, white arrow). On the other hand, we detected *type I collagen* expression in the surrounding membrane of the primordium (Fig. 5J, black arrows), implying that osteogenic differentiation was accelerated in *Myf5-Cre;Tgfbr2*$^{flox/flox}$ mice.

Normal migration of dorsal mesoderm-derived cells in *Myf5-Cre;Tgfbr2*$^{flox/flox}$ mice

Somites give rise to sclerotome and myotome, and then the cells in the dorsal sclerotome migrate to the dorsal midline (Christ et al., 2004; Christ et al., 2000). To assess the ability of mesoderm-derived cells from somites to migrate toward the dorsal midline, we collected early (E10.5) and middle (E13.5) gestation samples. Cell migration from the lateral to the dorsal area was indistinguishable in conditional knockout and control mice at E10.5 (Figs. 6A, B, arrowheads). At E13.5, cell migration was also normal in the primordia of both the supraoccipital bone and the neural arch of the C1 vertebra in conditional knockout mice (Figs. 6C-F), implying that the dorsal endochondral ossification defects in the *Myf5-Cre;Tgfbr2*$^{flox/flox}$ was not caused by abnormal migration of dorsal mesoderm-derived cells.

Compromised *Msx2* expression in the dorsal region of *Myf5-Cre;Tgfbr2*$^{flox/flox}$ mice

We compared the skull defects of *Myf5-Cre;Tgfbr2*$^{flox/flox}$ and *Msx* mutant mice, because *Msx1* and *Msx2* null mutants exhibit skull malformations (Chai et al., 2003; Satokata et al., 2000; Satokata and Maas, 1994). *Msx2* null mice have a supraoccipital bone defect, although the shape of the foramen magnum is unchanged from wild type (Figs. 3D, H, L, P).

NIH-PA Author Manuscript

NIH-PA Author Manuscript

NIH-PA Author Manuscript

Msx1 null mice exhibit normal formation of the supraoccipital bone (Figs. 3C, G, K) and the foramen magnum (Fig. 3O). Both *Mxs1* and *Msx2* null mice have normal formation of C1 vertebra (Figs. 3S, T). Although previous studies have shown that *Msx1* exhibits functional redundancy with the *Msx2* gene in some cases (Davidson, 1995; Ishii et al., 2005), our results suggest that only *Msx2* is involved in the formation of the supraoccipital bone. TGF-β may control *Msx2* gene expression to regulate supraoccipital bone development.

We next explored the molecular mechanism responsible for the caudal skull defects seen in the conditional knockout mice. *Msx1* and *Msx2* are critical factors for dorsoventral axis formation in vertebrae (Bach et al., 2003; Monsoro-Burq et al., 1994; Monsoro-Burq et al., 1996) and *Shh* induces the formation of ventral structures but inhibits the formation of dorsal structures (Monsoro-Burq et al., 1994; Takahashi et al., 1992). Based on our data, we hypothesized that *Msx* gene expression would be compromised in the dorsal area of *Tgfbr2* mutant mice. We found that the expression pattern of *Msx2* in the *Tgfbr2* sample was the same as that of the control mouse on the lateral side of embryo (Figs. 7A, B), but was diminished in the dorsal area from rostral to caudal (Figs. 7C, D, arrows). In contrast, the *Msx1* expression pattern in the conditional knockout mouse was indistinguishable from that of the control mouse (Figs. 7E-H). In addition, we observed no ectopic expression of *Shh* at the dorsal midline in the conditional knockout mouse (Figs. 7K, L). *Shh* was expressed at the tail bud and hind limb (Figs. 7I, J, arrows). Thus, TGF-β signaling does affect *Msx2* expression but it does not affect Shh signaling. Subsequently, we investigated whether *Msx2* was expressed in the supraoccipital primordium region at E12.5 when the undifferentiated mesoderm cells had begun to aggregate. In control mice, *Msx2* was expressed in aggregated cells from ventral to dorsal (Fig. 7M). However, the expression of *Msx2* was restricted to the ventral area containing a mixed population of LacZ positive and negative cells in conditional knockout mice (Fig. 7N, see Fig. 1C, arrow). The dorsal area of the supraoccipital primordium showed no *Msx2* expression (Fig. 7N).

To address further whether TGF-β might control *Msx2* gene expression in the mid-dorsal area, we performed bead implantation experiments at E10.5. TGF-β2 beads induced *Msx2* gene expression in control mice (Fig. 7O, black arrows). TGF-β1, however, did not induce *Msx2* gene expression (data not shown). In contrast, TGF-β2 failed to induce the expression of *Msx2* in conditional knockout mice (Fig. 7P). These results suggest that *Msx2* is a target gene of TGF-β2 in the mid-dorsal area.

Overexpression of *Msx2* rescues the supraoccipital bone defect of conditional knockout mice

If *Msx2* is a target gene of TGF-β signaling, *Msx2* overexpression might rescue defects in the *Myf5-Cre;Tgfbr2*$^{flox/flox}$ mice. To assess this possibility, we crossed *Msx2* transgenic mice (*Msx2*$^{Tg/+}$;*Tgfbr2*$^{flox/+}$), containing an exogenous *Msx2* promoter-driven *Msx2* gene (Liu et al., 1999), with *Myf5-Cre;Tgfbr2*$^{+/flox}$ mice. We confirmed that *Msx2* was overexpressed in *Msx2*$^{Tg/+}$;*Tgfbr2*$^{flox/+}$ mice using PCR (Fig. 8A). *Myf5-Cre;Tgfbr2*$^{flox/flox}$;*Msx2*$^{Tg/+}$ mice showed a hunchback phenotype similar to that of the *Myf5-Cre;Tgfbr2*$^{flox/flox}$ mice and microphthalmia, a phenotype of *Msx2*$^{Tg/+}$ mice (Fig. 8B) (Wu et al., 2003). However, we did not observe any hemorrhage around the occipital area in *Myf5-Cre;Tgfbr2*$^{flox/flox}$;*Msx2*$^{Tg/+}$ mice (Figs. 8C, D). Furthermore, we examined supraoccipital bone formation using bone staining and found that *Msx2* overexpression partially rescued that defect (N=2) (Figs. 8E, F, and see Fig. 3I). These results are consistent with a model in which the absence of TGF-β signaling causes decreased expression of *Msx*2 leading to the defect in the supraoccipital bone. Thus, overexpression of *Msx2* compensates for the lack of TGF-β during the development of the supraoccipital bone primordium. The rescue by *Msx2* was only partial, so TGF-β may also regulate other downstream target genes to control supraoccipital bone development.

NIH-PA Author Manuscript

NIH-PA Author Manuscript

NIH-PA Author Manuscript

Compromised cell proliferation in the supraoccipital bone primordium of *Myf5-Cre;Tgfbr2*$^{flox/flox}$ mice

To address whether there is a cell autonomous requirement for TGF-β signaling during supraoccipital bone development, we investigated cell proliferation in the perichondrium and cartilage tissues of the supraoccipital bone primordia at E12.5, E13.5, and E14.5. In control mice, musculature fiber formation started at E13.5 (Figs. 9A, C) and the fiber was well formed at E14.5 (Figs. 9G, I). In conditional knockout mice, we observed disorganization of the musculature fiber at E15.5, which had begun at E13.5 (Figs. 9B, D, H, J, white arrowhead). We also observed disorganization of the perichondrium at E15.5 in the conditional knockout mice (Fig. 5D), although this structure was similar to wild type at E13.5 and E14.5 (Figs. 9D, J, black arrow). We examined BrdU incorporation to determine whether cell proliferation might be decreased in the conditional knockout mice. At E12.5, the cell proliferation activity in control and conditional knockout mice was similar in the aggregated mesoderm cell region, which gives rise to the supraoccipital bone primordium (Fig. 9M). However, at E13.5 and E14.5, chondrocyte cell proliferation was decreased in the primordium of the supraoccipital bone in the *Myf5-Cre;Tgfbr2*$^{flox/flox}$ sample (Figs. 9E, F, M). In the perichondrium, proliferation activity was indistinguishable in control and conditional knockout mice at E13.5 (Fig. 9M). Interestingly, proliferative activity of the perichondrium decreased at E14.5 in control mice (Figs. 9K, M). In contrast, proliferation persisted at E14.5 in conditional knockout mice (Figs. 9L, M).

Discussion

The skull vault is constructed from two cell lineages, CNC- and mesoderm-derived cells (Jiang et al., 2002; Morriss-Kay and Wilkie, 2005). In this study, we have found that TGF-β signaling is specifically required in somite-derived bone structures, supraoccipital bone and C1 vertebra. TGF-β signaling controls chondrocyte proliferation and prevents premature cartilage differentiation to bone. Furthermore, loss of TGF-β signaling compromises the expression of *Msx2*, but not *Msx1*, during supraoccipital bone development. Significantly, overexpression of *Msx2* in *Myf5-Cre;Tgfbr2*$^{flox/flox}$ mutant mice partially rescues supraoccipital bone development. These findings suggest that TGF-β signaling-mediated *Msx2* expression is critical for somite-derived caudal skull development.

Occipital bone as evolutionary derivatives of vertebrae

Historically, Goethe first proposed a vertebral theory, in which the skull is a form of vertebra. More recently, evolutionary developmental biologists have suggested that the occipital bone is one of the vertebrae and the supraoccipital bone corresponds to the neural arch of the cervical vertebra (Kuratani, 2003; Olsson et al., 2005; Romer and Parsons, 1977). Chicken and quail experiments have demonstrated that mesoderm-derived cells contribute to the formation of occipital bone. The cells from somite 1 and 2 are distributed into supraoccipital bone, and the cells from somite 5 and 6 contribute to C1 vertebra (Huang et al., 2000). During embryonic development, these somite-derived cells form the dorsal sclerotome, which gives rise to the anlagen of the neural arch of vertebra (Christ et al., 2004; Dockter and Ordahl, 1998). It is unknown whether mesoderm-derived cells are distributed into the supraoccipital bone in mice. In our present study, somite-derived cells are LacZ positive (*Myf5* promoter-driven), but paraxial mesoderm cells are negative (see Fig. 1). Since paraxial mesoderm gives rise to parietal bone (our unpublished data), this explains why there is no defect in the formation of parietal bone in *Myf5-Cre;Tgfbr2*$^{flox/flox}$ mutant mice. Significantly, LacZ positive cells, which derive from somites, populate the primordia of the supraoccipital bone and C1 neural arch. Thus, we report for the first time that somite-derived cells can migrate into the anlage of the supraoccipital bone in the mouse embryo.

NIH-PA Author Manuscript

NIH-PA Author Manuscript

NIH-PA Author Manuscript

Furthermore, the supraoccipital bone is more closely related to the cervical vertebra than the rest of the skull in mice.

Msx genes are involved in the formation of the caudal skull

Chicken and quail experiments have revealed that *Msx* is a critical factor in the formation of the dorsoventral axis (Takahashi and Le Douarin, 1990; Takahashi et al., 1992). For instance, notochord explantation into the dorsal area results in the diminished expression of *Msx* genes in the dorsal area due to ectopic expression of *Shh* (Monsoro-Burq et al., 1994). Consequently, the reduced expression of *Msx* genes causes a defect of neural arch development in the dorsal area (Monsoro-Burq et al., 1994). Although *Msx1* and *Msx2* show functional redundancy in numerous tissues (Alappat et al., 2003), they have unique expression patterns and functions in specific areas. *Msx1* null mice have development defects such as cleft secondary palate, deficiency of the alveolar bone in the mandible and maxilla, and failure of tooth development (Satokata and Maas, 1994). On the other hand, *Msx2* null mice have defects in supraoccipital and frontal bone development (Satokata et al., 2000). Overexpression of *Msx2* in mice results in skull defects that mimic the phenotype of human Boston-type craniosynostosis (Liu et al., 1995; Liu et al., 1999). These findings suggest that each *Msx* gene possesses a specific expression pattern and plays a unique role in regulating craniofacial development. In this study, we conclude that *Msx2* possesses an important function in supraoccipital bone formation. Compromised *Msx2* gene expression is likely to be at least partly responsible for the supraoccipital bone defect in the *Tgfbr2* conditional knockout mouse, because overexpression of *Msx2* in the *Myf5-Cre;Tgfbr2*$^{flox/flox}$ mice results in the partial rescue of supraoccipital bone development.

TGF-β controls *Msx2* expression in presumptive supraoccipital bone primordia

As mentioned before, *Msx2* null mice show intramembranous and endochondral ossification defects (Satokata et al., 2000), and the number of chondrocytes in their resting, proliferating, and hypertrophic zones is decreased. In our present study, cell numbers in these three zones are also decreased, suggesting that TGF-β signaling is involved in chondrogenesis by controlling *Msx2* expression in undifferentiated cells that give rise to endochondral bone. Previous studies have suggested that *Msx2* represses chondrogenesis without causing cell death (Takahashi et al., 2001). Interestingly, *Sox9*, a gene involved in chondrocyte differentiation, is co-expressed with *Msx2* in cranial neural crest cells. *Msx2* expression is tightly linked to the expression of Sox9 around the area of cartilage differentiation (Semba et al., 2000). The lack of *Msx2* in the supraoccipital bone primordium of *Tgfbr2* conditional knockout mice might result in the loss of a chondrocyte differentiation repressor. Consequently, chondrocyte differentiation is accelerated in mesoderm-derived cells in the *Myf5-Cre;Tgfbr2*$^{flox/flox}$ mouse.

TGF-β signaling regulates the expression of transcription factors, which in turn regulate the fate of CNC cells by controlling the progression of the cell cycle (Han et al., 2003; Ito et al., 2003; Moses and Serra, 1996). For example, TGF-β controls the expression of *Msx1* in the CNC-derived palatal mesenchyme prior to palatal fusion (Ito et al., 2003). BMP, a member of the TGF-β family, is known to regulate *Msx2* expression to control the fate of CNC cells during craniofacial development (Brugger et al., 2004; Liu et al., 2005). In this study, we discovered that TGF-β-mediated *Msx2* expression is critical for regulating the mesoderm-derived cells that contribute to the development of the caudal region of skull. Clearly, members of the TGF-β family play important roles in regulating *Msx* gene expression during craniofacial development. Specific TGF-β/BMP and Msx1/Msx2 regulatory interactions may help to set up temporal and spatial specificity to achieve diverse developmental outcomes during craniofacial morphogenesis. It is important to point out that the lack of a completely rescued supraoccipital bone development in *Myf5-*

NIH-PA Author Manuscript

NIH-PA Author Manuscript

NIH-PA Author Manuscript

Cre;Tgfbr2$^{flox/flox}$;*Msx2*$^{Tg/+}$ mice suggests that, in addition to *Msx2*, TGF-β regulates the expression of other factors, underscoring the complicated nature of the TGF-β signaling network in regulating craniofacial morphogenesis.

TGF-β possesses an autonomous function for chondrocyte differentiation in endochondral ossification

TGF-β plays an important role in regulating chondrocyte proliferation and differentiation. The conditional inactivation of Smad4, a TGF-β signaling mediator, causes decreased cell proliferation and the maturation of chondrocytes (Zhang et al., 2005). The maturation of chondrocytes is also faster in dominant negative TGF-β type II receptor mice than wild-type mice. Consequently, dominant negative mice develop a degenerative joint disease resembling osteoarthritis in humans (Serra et al., 1997). *Col2a-Cre;Tgfbr2*$^{flox/flox}$ mice, which lack *Tgfbr2* specifically in chondrocytes, show normal long bone formation. However, occipital bones, formed by endochondral ossification, exhibit malformations in these mutant mice (Baffi et al., 2004). It is controversial whether TGF-β possesses an autonomous function in chondrocytes or a non-autonomous function whereby it affects chondrocytes through signaling in the perichondrium. In the non-autonomous model, TGF-β is required in the perichondrium to control the expression of Ihh and PTHrP in cartilage (Alvarez et al., 2001; Alvarez et al., 2002). Ihh and PTHrP are then required to inhibit the differentiation of chondrocytes. However, Ihh/PTHrP signaling inhibits the hypertrophic differentiation of chondrocytes independently of Smad4-mediated TGF-β signals in *Cola2-Cre;Smad4*$^{flox/flox}$ conditional knockout mice (Zhang et al., 2005). Studies with *Cola2-Cre;Smad4*$^{flox/flox}$ mice also show that TGF-β has an autonomous function to control the cell proliferation and differentiation of chondrocytes. The present study demonstrates that compromised TGF-β signaling within the cartilage results in decreased proliferation of chondrocytes and accelerated differentiation in the *Myf5-Cre;Tgfbr2*$^{flox/flox}$ mutant. As chondrocytes in the *Tgfbr2* mutant have lost their ability to respond to TGF-β signaling, our results support a model in which TGF-β possesses an autonomous function to inhibit chondrocyte differentiation.

Supplementary Material

Refer to Web version on PubMed Central for supplementary material.

Acknowledgments

We thank Julie Mayo, Mamoru Ishii, and Brauch Frenkel for critical reading of the manuscript. We also thank J. L. R. Rubenstein for reagents; H. Moses for the *Tgfbr2*$^{fl/fl}$ mice, Philippe Soriano for *Myf5-Cre* and Rob Maxson for *Msx2*$^{TG/+}$ mice. This study was supported by grants from the National Institute of Dental and Craniofacial Research, NIH (DE017007, DE012711, and DE014078) and March of Dimes Birth Defect Foundation (#6-FY05-67) to Yang Chai.

References

Alappat S, Zhang ZY, Chen YP. Msx homeobox gene family and craniofacial development. Cell Res. 2003; 13:429–442. [PubMed: 14728799]

Alvarez J, Horton J, Sohn P, Serra R. The perichondrium plays an important role in mediating the effects of TGF-beta1 on endochondral bone formation. Dev Dyn. 2001; 221:311–321. [PubMed: 11458391]

Alvarez J, Sohn P, Zeng X, Doetschman T, Robbins DJ, Serra R. TGFbeta2 mediates the effects of hedgehog on hypertrophic differentiation and PTHrP expression. Development. 2002; 129:1913–1924. [PubMed: 11934857]

Bach A, Lallemand Y, Nicola MA, Ramos C, Mathis L, Maufras M, Robert B. Msx1 is required for dorsal diencephalon patterning. Development. 2003; 130:4025–4036. [PubMed: 12874124]

NIH-PA Author Manuscript

NIH-PA Author Manuscript

NIH-PA Author Manuscript

Baffi MO, Slattery E, Sohn P, Moses HL, Chytil A, Serra R. Conditional deletion of the TGF-beta type II receptor in Col2a expressing cells results in defects in the axial skeleton without alterations in chondrocyte differentiation or embryonic development of long bones. Dev Biol. 2004; 276:124–142. [PubMed: 15531369]

Braun T, Rudnicki MA, Arnold HH, Jaenisch R. Targeted inactivation of the muscle regulatory gene Myf-5 results in abnormal rib development and perinatal death. Cell. 1992; 71:369–382. [PubMed: 1423602]

Brugger SM, Merrill AE, Torres-Vazquez J, Wu N, Ting MC, Cho JY, Dobias SL, Yi SE, Lyons K, Bell JR, Arora K, Warrior R, Maxson R. A phylogenetically conserved cis-regulatory module in the Msx2 promoter is sufficient for BMP-dependent transcription in murine and Drosophila embryos. Development. 2004; 131:5153–5165. [PubMed: 15459107]

Chai Y, Ito Y, Han J. TGF-beta signaling and its functional significance in regulating the fate of cranial neural crest cells. Crit Rev Oral Biol Med. 2003; 14:78–88. [PubMed: 12764071]

Chai Y, Jiang X, Ito Y, Bringas P Jr, Han J, Rowitch DH, Soriano P, McMahon AP, Sucov HM. Fate of the mammalian cranial neural crest during tooth and mandibular morphogenesis. Development. 2000; 127:1671–1679. [PubMed: 10725243]

Chai Y, Mah A, Crohin C, Groff S, Bringas P Jr, Le T, Santos V, Slavkin HC. Specific transforming growth factor-beta subtypes regulate embryonic mouse Meckel's cartilage and tooth development. Dev Biol. 1994; 162:85–103. [PubMed: 8125201]

Christ B, Huang R, Scaal M. Formation and differentiation of the avian sclerotome. Anat Embryol (Berl). 2004; 208:333–350. [PubMed: 15309628]

Christ B, Huang R, Wilting J. The development of the avian vertebral column. Anat Embryol (Berl). 2000; 202:179–194. [PubMed: 10994991]

Chytil A, Magnuson MA, Wright CV, Moses HL. Conditional inactivation of the TGF-beta type II receptor using Cre:Lox. Genesis. 2002; 32:73–75. [PubMed: 11857781]

Couly GF, Coltey PM, Le Douarin NM. The triple origin of skull in higher vertebrates: a study in quail-chick chimeras. Development. 1993; 117:409–429. [PubMed: 8330517]

Davidson D. The function and evolution of Msx genes: pointers and paradoxes. Trends Genet. 1995; 11:405–411. [PubMed: 7482767]

Dockter JL, Ordahl CP. Determination of sclerotome to the cartilage fate. Development. 1998; 125:2113–2124. [PubMed: 9570775]

Dunker N, Krieglstein K. Tgfbeta2 -/- Tgfbeta3 -/- double knockout mice display severe midline fusion defects and early embryonic lethality. Anat Embryol (Berl). 2002; 206:73–83. [PubMed: 12478370]

Grass S, Arnold HH, Braun T. Alterations in somite patterning of Myf-5-deficient mice: a possible role for FGF-4 and FGF-6. Development. 1996; 122:141–150. [PubMed: 8565825]

Han J, Ito Y, Yeo JY, Sucov HM, Maas R, Chai Y. Cranial neural crest-derived mesenchymal proliferation is regulated by Msx1-mediated p19(INK4d) expression during odontogenesis. Dev Biol. 2003; 261:183–196. [PubMed: 12941628]

Heyer J, Escalante-Alcalde D, Lia M, Boettinger E, Edelmann W, Stewart CL, Kucherlapati R. Postgastrulation Smad2-deficient embryos show defects in embryo turning and anterior morphogenesis. Proc Natl Acad Sci U S A. 1999; 96:12595–12600. [PubMed: 10535967]

Hosokawa R, Urata MM, Ito Y, Bringas P Jr, Chai Y. Functional significance of Smad2 in regulating basal keratinocyte migration during wound healing. J Invest Dermatol. 2005; 125:1302–1309. [PubMed: 16354202]

Huang R, Zhi Q, Patel K, Wilting J, Christ B. Contribution of single somites to the skeleton and muscles of the occipital and cervical regions in avian embryos. Anat Embryol (Berl). 2000; 202:375–383. [PubMed: 11089929]

Hui CC, Joyner AL. A mouse model of greig cephalopolysyndactyly syndrome: the extra-toesJ mutation contains an intragenic deletion of the Gli3 gene. Nat Genet. 1993; 3:241–246. [PubMed: 8387379]

Ishii M, Han J, Yen HY, Sucov HM, Chai Y, Maxson RE Jr. Combined deficiencies of Msx1 and Msx2 cause impaired patterning and survival of the cranial neural crest. Development. 2005; 132:4937–4950. [PubMed: 16221730]

NIH-PA Author Manuscript

NIH-PA Author Manuscript

NIH-PA Author Manuscript

Ishii M, Merrill AE, Chan YS, Gitelman I, Rice DP, Sucov HM, Maxson RE Jr. Msx2 and Twist cooperatively control the development of the neural crest-derived skeletogenic mesenchyme of the murine skull vault. Development. 2003; 130:6131–6142. [PubMed: 14597577]

Ito Y, Yeo JY, Chytil A, Han J, Bringas P Jr, Nakajima A, Shuler CF, Moses HL, Chai Y. Conditional inactivation of Tgfbr2 in cranial neural crest causes cleft palate and calvaria defects. Development. 2003; 130:5269–5280. [PubMed: 12975342]

Jiang X, Iseki S, Maxson RE, Sucov HM, Morriss-Kay GM. Tissue origins and interactions in the mammalian skull vault. Dev Biol. 2002; 241:106–16. [PubMed: 11784098]

Kuratani S. Evolutionary development biology and vertebrae head segmentation: a perspective from develomental constraint. Theor Biosci. 2003; 122:230–251.

Kuratani S. Craniofacial development and the evolution of the vertebrates: the old problems on a new background. Zoolog Sci. 2005; 22:1–19. [PubMed: 15684579]

Liu W, Selever J, Murali D, Sun X, Brugger SM, Ma L, Schwartz RJ, Maxson R, Furuta Y, Martin JF. Threshold-specific requirements for Bmp4 in mandibular development. Dev Biol. 2005; 283:282–293. [PubMed: 15936012]

Liu YH, Kundu R, Wu L, Luo W, Ignelzi MA Jr, Snead ML, Maxson RE Jr. Premature suture closure and ectopic cranial bone in mice expressing Msx2 transgenes in the developing skull. Proc Natl Acad Sci U S A. 1995; 92:6137–6141. [PubMed: 7597092]

Liu YH, Tang Z, Kundu RK, Wu L, Luo W, Zhu D, Sangiorgi F, Snead ML, Maxson RE. Msx2 gene dosage influences the number of proliferative osteogenic cells in growth centers of the developing murine skull: a possible mechanism for MSX2-mediated craniosynostosis in humans. Dev Biol. 1999; 205:260–274. [PubMed: 9917362]

McLeod MJ. Differential staining of cartilage and bone in whole mouse fetuses by alcian blue and alizarin red S. Teratology. 1980; 22:299–301. [PubMed: 6165088]

Monsoro-Burq AH, Bontoux M, Teillet MA, Le Douarin NM. Heterogeneity in the development of the vertebra. Proc Natl Acad Sci U S A. 1994; 91:10435–10439. [PubMed: 7937970]

Monsoro-Burq AH, Duprez D, Watanabe Y, Bontoux M, Vincent C, Brickell P, Le Douarin N. The role of bone morphogenetic proteins in vertebral development. Development. 1996; 122:3607–3616. [PubMed: 8951076]

Morriss-Kay GM. Derivation of the mammalian skull vault. J Anat. 2001; 199:143–151. [PubMed: 11523816]

Morriss-Kay GM, Wilkie AO. Growth of the normal skull vault and its alteration in craniosynostosis: insights from human genetics and experimental studies. J Anat. 2005; 207:637–653. [PubMed: 16313397]

Moses HL, Serra R. Regulation of differentiation by TGF-beta. Curr Opin Genet Dev. 1996; 6:581–586. [PubMed: 8939725]

Noden DM. Interactions and fates of avian craniofacial mesenchyme. Development. 1988; 103(Suppl): 121–140. [PubMed: 3074905]

Noden DM, Trainor PA. Relations and interactions between cranial mesoderm and neural crest populations. J Anat. 2005; 207:575–601. [PubMed: 16313393]

Nomura M, Li E. Smad2 role in mesoderm formation, left-right patterning and craniofacial development. Nature. 1998; 393:786–790. [PubMed: 9655392]

Olsson L, Ericsson R, Cerny R. Vertebrate head development: Segmentation, novelties, and homology. Theor Biosci. 2005; 124:145–163.

Oshima M, Oshima H, Taketo MM. TGF-beta receptor type II deficiency results in defects of yolk sac hematopoiesis and vasculogenesis. Dev Biol. 1996; 179:297–302. [PubMed: 8873772]

Ott MO, Bober E, Lyons G, Arnold H, Buckingham M. Early expression of the myogenic regulatory gene, myf-5, in precursor cells of skeletal muscle in the mouse embryo. Development. 1991; 111:1097–1107. [PubMed: 1652425]

Romer, S.; Parsons, S. The vertebrate body. W. B. Saunders company; Philadelphia: 1977.

Sanford LP, Ormsby I, Gittenberger-de Groot AC, Sariola H, Friedman R, Boivin GP, Cardell EL, Doetschman T. TGFbeta2 knockout mice have multiple developmental defects that are non-overlapping with other TGFbeta knockout phenotypes. Development. 1997; 124:2659–2670. [PubMed: 9217007]

NIH-PA Author Manuscript

NIH-PA Author Manuscript

NIH-PA Author Manuscript

Sasaki T, Ito Y, Bringas P Jr, Chou S, Urata MM, Slavkin H, Chai Y. TGF{beta}-mediated FGF signaling is crucial for regulating cranial neural crest cell proliferation during frontal bone development. Development. 2006; 133:371–381. [PubMed: 16368934]

Satokata I, Ma L, Ohshima H, Bei M, Woo I, Nishizawa K, Maeda T, Takano Y, Uchiyama M, Heaney S, Peters H, Tang Z, Maxson R, Maas R. Msx2 deficiency in mice causes pleiotropic defects in bone growth and ectodermal organ formation. Nat Genet. 2000; 24:391–395. [PubMed: 10742104]

Satokata I, Maas R. Msx1 deficient mice exhibit cleft palate and abnormalities of craniofacial and tooth development. Nat Genet. 1994; 6:348–356. [PubMed: 7914451]

Semba I, Nonaka K, Takahashi I, Takahashi K, Dashner R, Shum L, Nuckolls GH, Slavkin HC. Positionally-dependent chondrogenesis induced by BMP4 is co-regulated by Sox9 and Msx2. Dev Dyn. 2000; 217:401–414. [PubMed: 10767084]

Serra R, Johnson M, Filvaroff EH, LaBorde J, Sheehan DM, Derynck R, Moses HL. Expression of a truncated, kinase-defective TGF-beta type II receptor in mouse skeletal tissue promotes terminal chondrocyte differentiation and osteoarthritis. J Cell Biol. 1997; 139:541–552. [PubMed: 9334355]

Soriano P. Generalized lacZ expression with the ROSA26 Cre reporter strain. Nat Genet. 1999; 21:70–71. [PubMed: 9916792]

Stickens D, Behonick DJ, Ortega N, Heyer B, Hartenstein B, Yu Y, Fosang AJ, Schorpp-Kistner M, Angel P, Werb Z. Altered endochondral bone development in matrix metalloproteinase 13-deficient mice. Development. 2004; 131:5883–5895. [PubMed: 15539485]

Tajbakhsh S, Rocancourt D, Buckingham M. Muscle progenitor cells failing to respond to positional cues adopt non-myogenic fates in myf-5 null mice. Nature. 1996; 384:266–270. [PubMed: 8918877]

Takahashi K, Nuckolls GH, Takahashi I, Nonaka K, Nagata M, Ikura T, Slavkin HC, Shum L. Msx2 is a repressor of chondrogenic differentiation in migratory cranial neural crest cells. Dev Dyn. 2001; 222:252–262. [PubMed: 11668602]

Takahashi Y, Le Douarin N. cDNA cloning of a quail homeobox gene and its expression in neural crest-derived mesenchyme and lateral plate mesoderm. Proc Natl Acad Sci U S A. 1990; 87:7482–7486. [PubMed: 1977161]

Takahashi Y, Monsoro-Burq AH, Bontoux M, Le Douarin NM. A role for Quox-8 in the establishment of the dorsoventral pattern during vertebrate development. Proc Natl Acad Sci U S A. 1992; 89:10237–10241. [PubMed: 1359537]

Tallquist MD, Weismann KE, Hellstrom M, Soriano P. Early myotome specification regulates PDGFA expression and axial skeleton development. Development. 2000; 127:5059–5070. [PubMed: 11060232]

Weintraub H, Davis R, Tapscott S, Thayer M, Krause M, Benezra R, Blackwell TK, Turner D, Rupp R, Hollenberg S, et al. The myoD gene family: nodal point during specification of the muscle cell lineage. Science. 1991; 251:761–766. [PubMed: 1846704]

Wilkinson, DG. In Situ Hybridaization: A Practical Approach. Oxford University Press; Oxford, UK: 1998.

Wu LY, Li M, Hinton DR, Guo L, Jiang S, Wang JT, Zeng A, Xie JB, Snead M, Shuler C, Maxson RE Jr, Liu YH. Microphthalmia resulting from MSX2-induced apoptosis in the optic vesicle. Invest Ophthalmol Vis Sci. 2003; 44:2404–2412. [PubMed: 12766037]

Yin T, Li L. The stem cell niches in bone. J Clin Invest. 2006; 116:1195–1201. [PubMed: 16670760]

Zhang J, Tan X, Li W, Wang Y, Wang J, Cheng X, Yang X. Smad4 is required for the normal organization of the cartilage growth plate. Dev Biol. 2005; 284:311–322. [PubMed: 16023633]

NIH-PA Author Manuscript
NIH-PA Author Manuscript
NIH-PA Author Manuscript

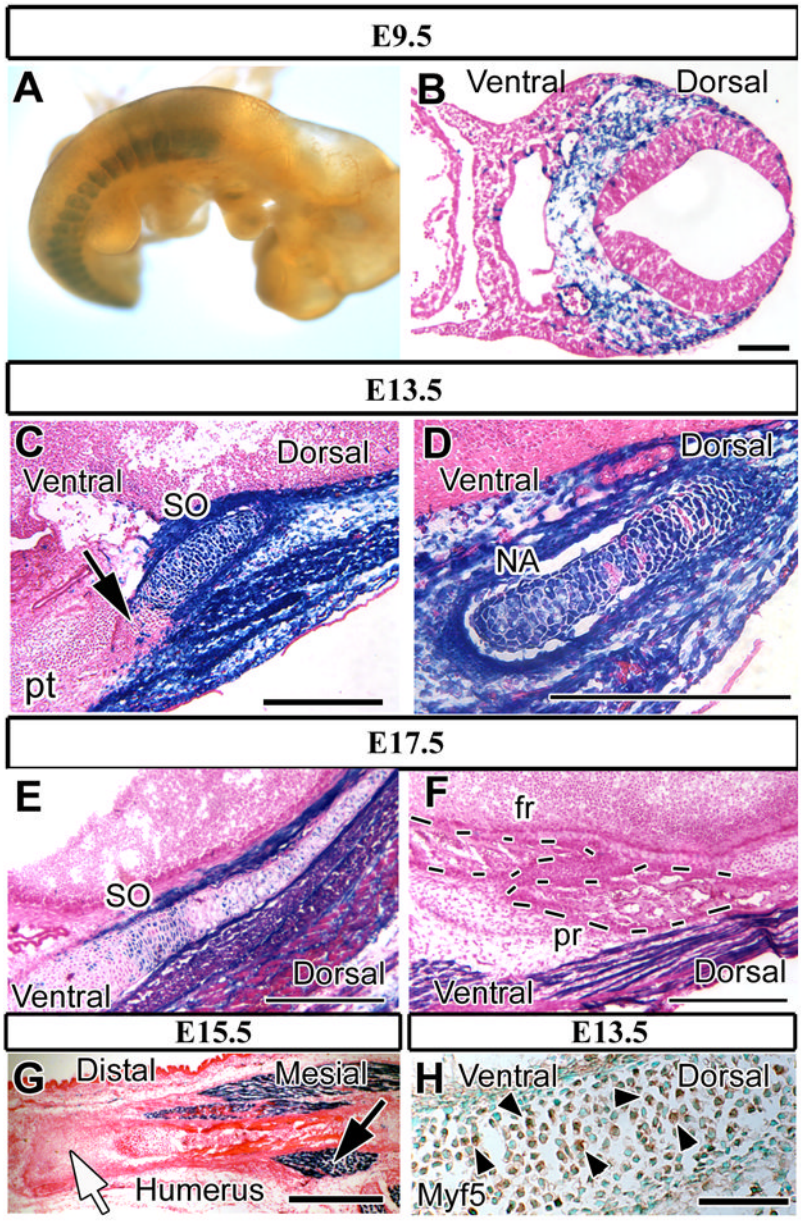

Figure 1. Mesoderm-derived structures are positive for *Myf5*-directed expression of lacZ

Lateral view of lacZ staining (blue) of *Myf5-Cre;R26R*$^{flox/+}$ whole-mount E9.5 samples (A) and cross sections of E9.5 (B), E13.5 (C, D), E15.5 (G) and E17.5 samples (E, F). (A) LacZ staining is detectable in somites but not the paraxial mesoderm cells in the craniofacial region. (B) Mesoderm-derived cells in the occipital somite area show lacZ expression. (C, D) The primordia of the supraoccipital bone (SO) and the neural arch of C1 (C1) are populated by lacZ positive somite–derived cells. Non-blue cells are visible in the ventral area of the SO and the cartilage primordium of the petrous part of the temporal bone (pt) (C, black arrow). (E) Chondrocytes in the supraoccipital bone are lacZ positive. (F) Cells in the parietal bone (pr) and frontal bone (fr) (dashed line) are negative for lacZ staining. (G) Chondrocytes and osteoblasts in the humerus are lacZ negative (white arrow). Myogenic cells are LacZ positive around the humerus (black arrow). (H) Myf5 immunostaining of E13.5 *Myf5-Cre;R26R*$^{flox/+}$ mice. Chondrocytes in the supraoccipital

bone primordium are positive for Myf5 (arrowheads). Scale bars: 100 μm in B, 500 μm in C-D, 300 μm in E-G, 50 μm in H.

NIH-PA Author Manuscript
NIH-PA Author Manuscript
NIH-PA Author Manuscript

NIH-PA Author Manuscript
NIH-PA Author Manuscript
NIH-PA Author Manuscript

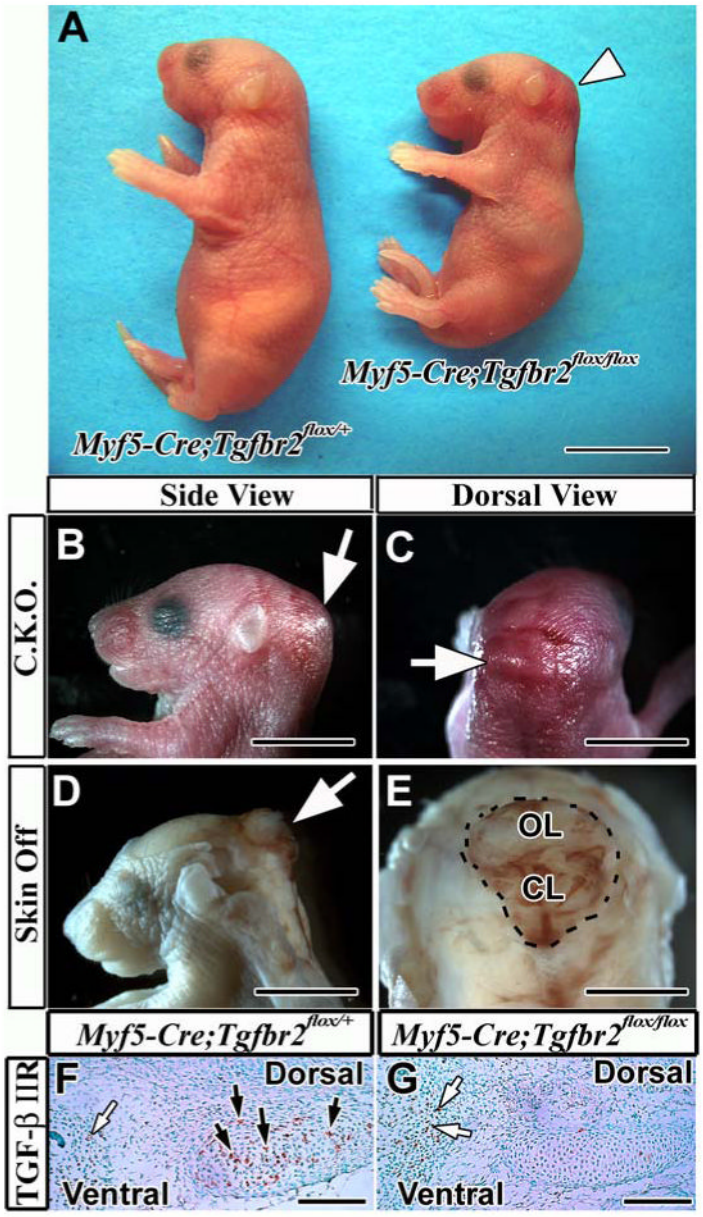

Figure 2. *Myf5-Cre;Tgfbr2*$^{flox/flox}$ mouse pups show altered posture and meningoencephalocele in the occipital area

(A) *Myf5-Cre;Tgfbr2*$^{flox/flox}$ mice (right) display a hunchback phenotype and hemorrhage in the occipital area (white arrowhead). (B, C) Swelling is associated with the hemorrhage in the occipital area (white arrow) in the conditional knockout mouse (C.K.O.). (D, E) Peeling the skin above the swelling area reveals the excrescence of the brain in the occipital area (white arrows). (F, G) Immunostaining of TGF-β type II receptor in the supraoccipital bone primordium of *Myf5-Cre;Tgfbr2*$^{flox/+}$ (F) and *Myf5-Cre;Tgfbr2*$^{flox/flox}$ (G) mice. Brown color indicates TGF-β type II receptor expression in the supraoccipital bone primordium (black arrows). White arrows indicate immunopositive cells in the lacZ negative area (see figure 1C). Abbreviations: CL, cerebellum; OL, occipital lobe. Scale bars: 1 cm in A, 5 mm in B-E, 100 μm in F, G.

NIH-PA Author Manuscript
NIH-PA Author Manuscript
NIH-PA Author Manuscript

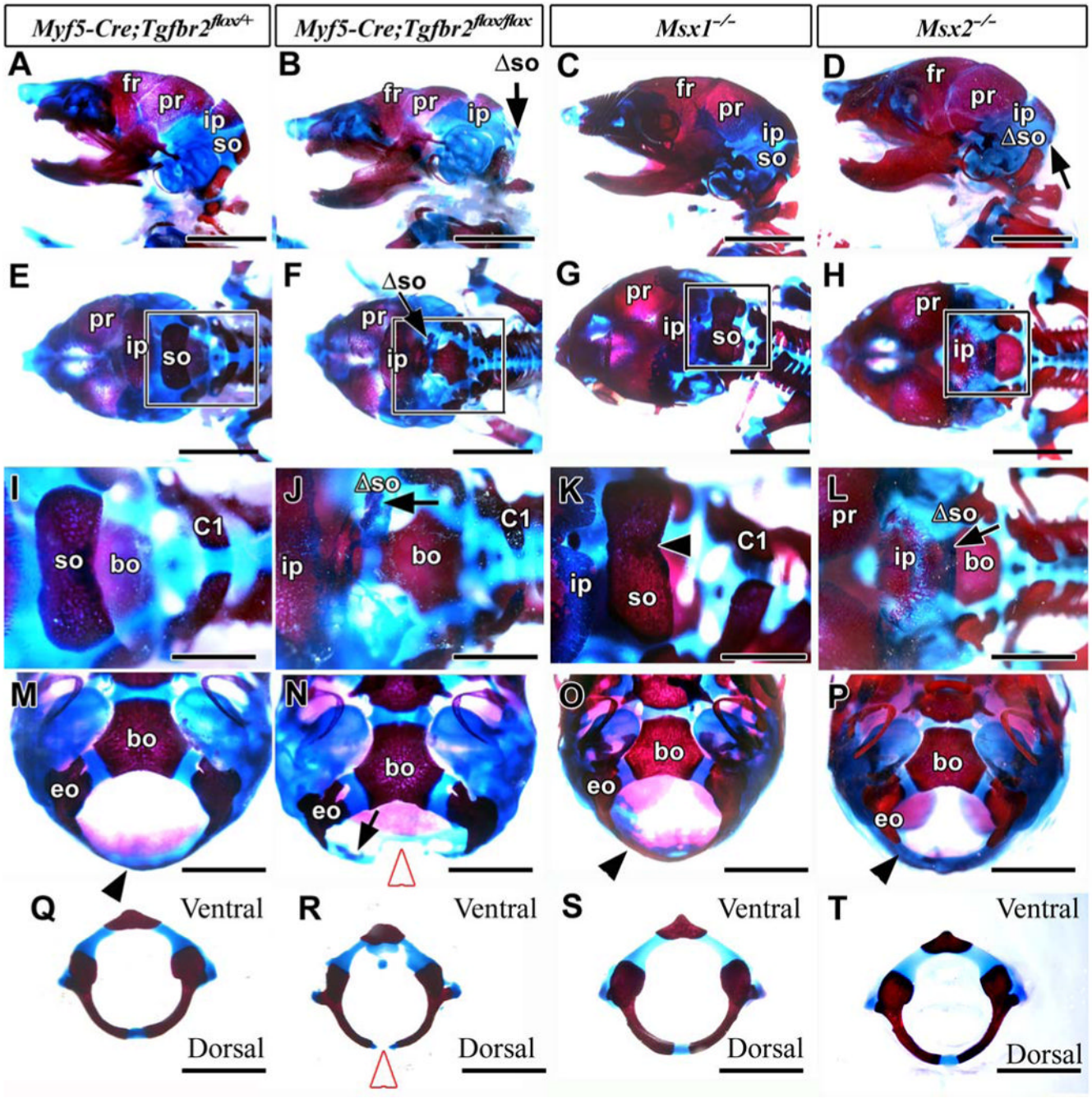

Figure 3. Supraoccipital bone defect in *Myf5-Cre;Tgfbr2*$^{flox/flox}$ newborn pups

Alizarin red/Alcian blue-stained skeletons of *Myf5-Cre;Tgfbr2*$^{flox/+}$ (control; A, E, I, M, Q), *Myf5-Cre;Tgfbr2*$^{flox/flox}$ (B, F, J, N, R), *Msx1*$^{-/-}$ (C, G, K, O, S), and *Msx2*$^{-/-}$ (D, H, L, P, T) mice, showing side (A-D), dorsal (E-L), and ventral (M-P) views and C1 vertebrae (Q-T). I, J, K, and L are enlarged from the boxes of E, F, G, and H, respectively.

(A, E) The control mouse contains a frontal (fr), parietal (pr), interparietal (ip), and supraoccipital bone (so). (B, F, J, N) The supraoccipital bone of the conditional knockout mouse is hypomorphic (Λso, black arrow). (C, G, K) The *Msx1*$^{-/-}$ mouse shows normal development of the supraoccipital bone. (D, H, L) The *Msx2*$^{-/-}$ mouse shows a diminished supraoccipital bone (Λso, black arrow). (M) The occipital bone surrounding the foramen

magnum dorsally (black arrowhead) is continuous in the control mouse. (N) The conditional knockout mouse shows a gap in the dorsal portion of occipital bone (white arrowhead) and a diminished supraoccipital bone (black arrow). (O, P) The *Msx1*$^{-/-}$ and *Msx2*$^{-/-}$ mice have continuous occipital bones forming the foramen magnum (black arrowheads). (Q, R) The conditional knockout mouse shows a disconnection dorsally in the neural arch of the C1 vertebra (white arrowhead). (S, T) The C1 vertebrae in both *Msx1*$^{-/-}$ and *Msx2*$^{-/-}$ mice appear normal. Abbreviations: bo, basioccipital bone; C1, the neural arch of first cervical vertebra; eo, exoccipital bone. Scale bars: 5 mm in A-H, 2 mm in I-T.

NIH-PA Author Manuscript
NIH-PA Author Manuscript
NIH-PA Author Manuscript

NIH-PA Author Manuscript
NIH-PA Author Manuscript
NIH-PA Author Manuscript

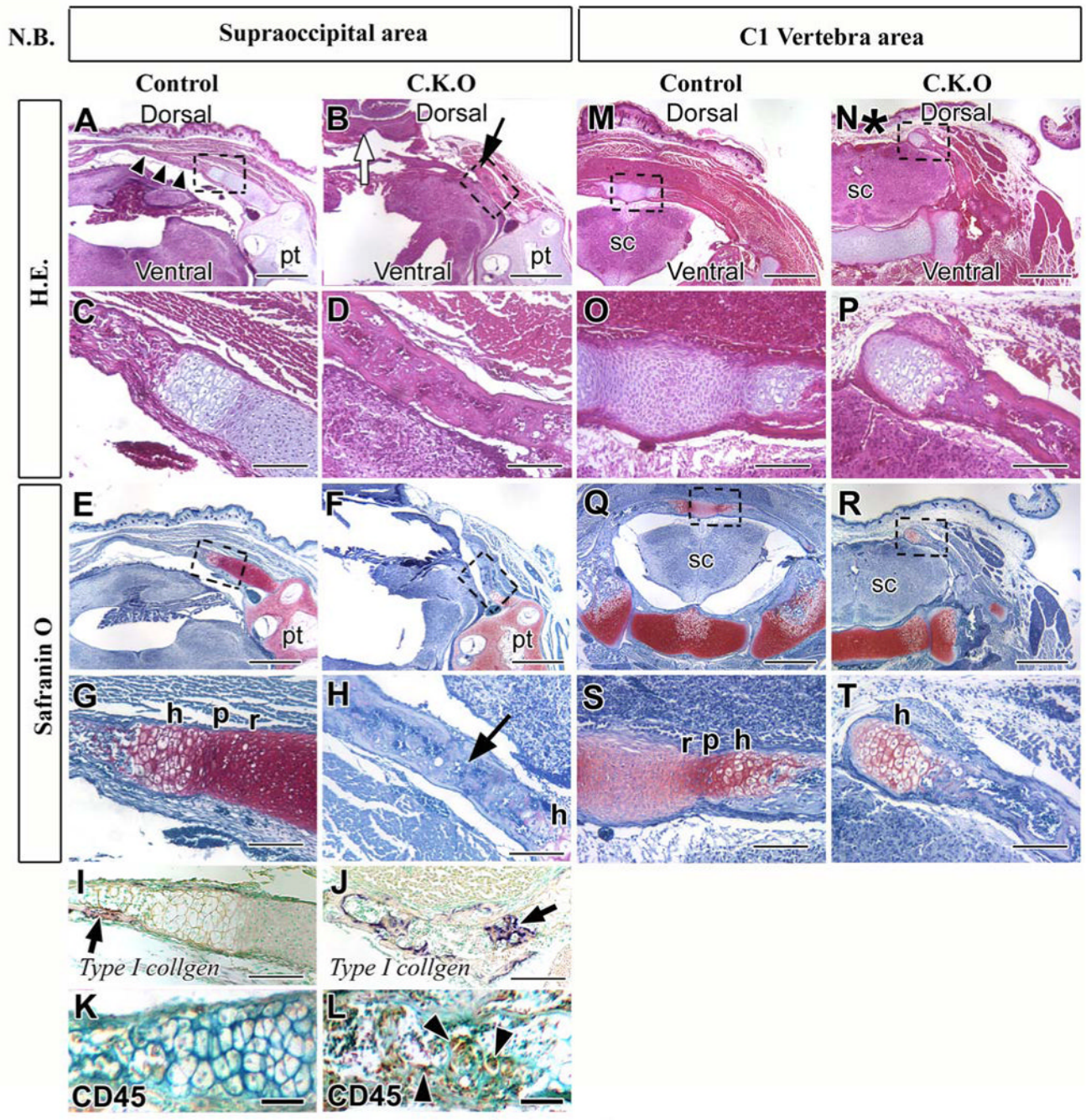

Figure 4. The supraoccipital bone and the C1 vertebra fail to fuse in the mid-dorsal area in *Myf5-Cre;Tgfbr2*$^{flox/flox}$ newborn mice

Hematoxylin and Eosin (H.E.) staining (A-D, M-P) and Safranin O staining (E-H, Q-T) of cross sections from the supraoccipital bone (A-L), and the neural arch of C1 vertebra (M-T) in control and *Myf5-Cre;Tgfbr2*$^{flox/flox}$ mice (C.K.O.). C, D, G, H, O, P, S, T are enlarged areas from the boxes in A, B, E, F, M, N, Q, and R, respectively.

(A, C) The supraoccipital bone of control mice extends to the mid-dorsal area (black arrowheads) and contains cartilage structure at the base of the bone. (B, D) and *Myf5-Cre;Tgfbr2*$^{flox/flox}$ mice have a shorter extension of the supraoccipital bone (arrow indicates the edge of bone) and a conversion of cartilage into bone structure. Part of the brain is

NIH-PA Author Manuscript

NIH-PA Author Manuscript

NIH-PA Author Manuscript

outside the skull vault (B, white arrow). (E, G) The cartilage in the supraoccipital bone base of control mice contains hypertrophic (h), proliferating (p), and resting (r) zones. (F, H) The base of the supraoccipital bone in the conditional knockout mice contains only a small hypertrophic zone, and the remainder is replaced by bone tissue (black arrow). (I, J) *Type I collagen* expression in the supraoccipital bone of control (I) and *Myf5-Cre;Tgfbr2*$^{flox/flox}$ (J) mice (black arrows). (K, L) Immunostaining of CD45, a marker of hematopoietic cells, in control (K) and *Myf5-Cre;Tgfbr2*$^{flox/flox}$ (L) mice. CD45 positive cells (brown color, arrowheads) are detectable adjacent to bone in the *Myf5-Cre;Tgfbr2*$^{flox/flox}$ sample. (M, O) The right and left sides of the neural arch of C1 vertebra are connected with cartilage mid-dorsally in the control mice. (N, P) The neural arch of C1 vertebra in *Myf5-Cre;Tgfbr2*$^{flox/flox}$ mice does not extend to the dorsal midline (asterisk). (Q, S) The mid-dorsal cartilage of control mice contains hypertrophic (h), proliferating (p), and resting (r) zones. (R, T) The edge of the neural arch, which does not extend to the midline, contains only a hypertrophic zone in the and *Myf5-Cre;Tgfbr2*$^{flox/flox}$ mice. Abbreviations: pt, petrous part of temporal bone; sc, spinal cord. Scale bars: 500 μm in A, B, E, F, M, N, Q, R, 300 μm in C, D, G, H, I, J, O, P, S, T, 50 μm in K, L.

NIH-PA Author Manuscript
NIH-PA Author Manuscript
NIH-PA Author Manuscript

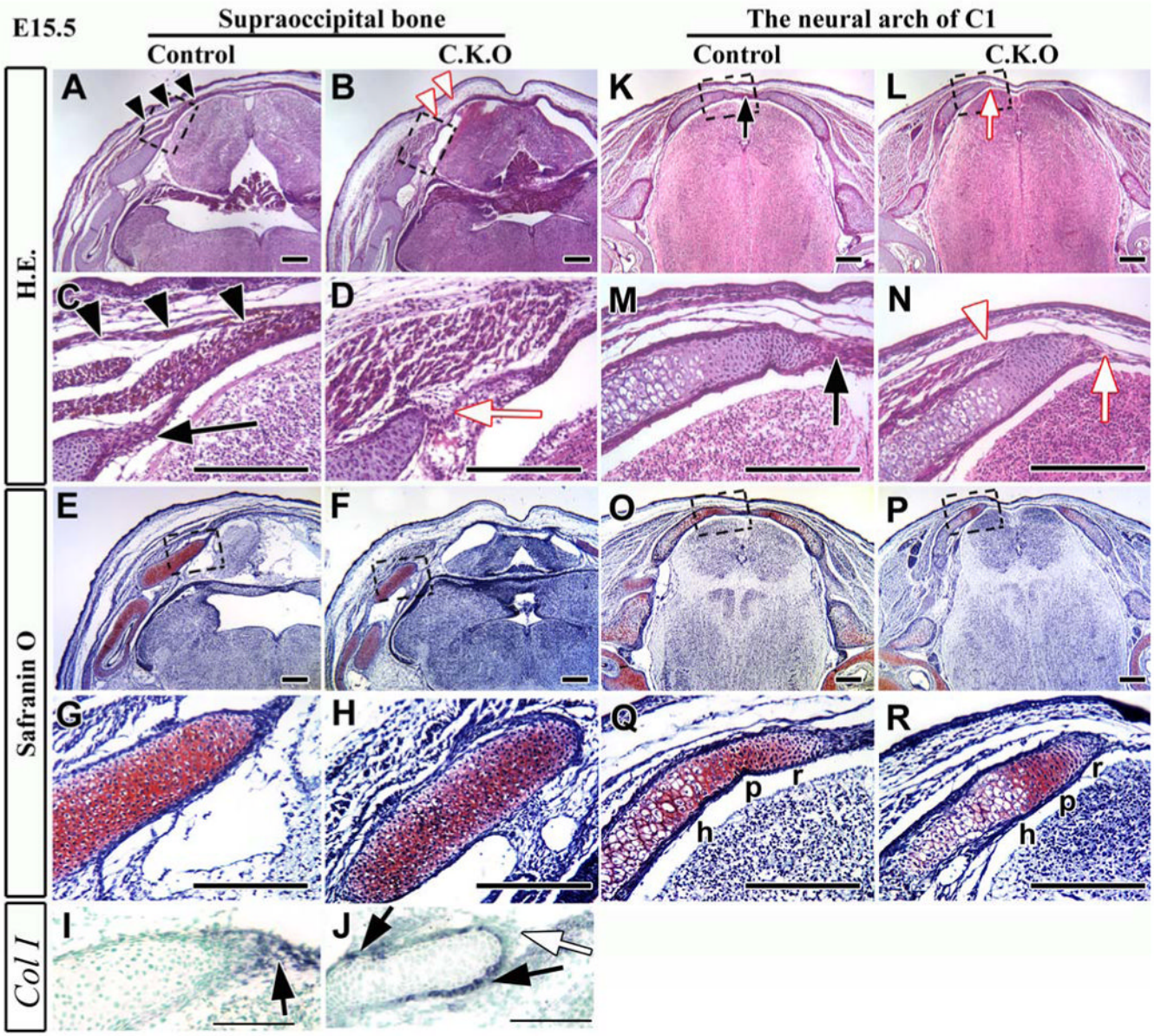

Figure 5. Development of cartilage and muscle tissue is compromised in the mid-dorsal region of *Myf5-Cre;Tgfbr2*$^{flox/flox}$ mice

Hematoxylin and Eosin (A-D, K-N) and Safranin O (E-H, O-R) staining of cross-sections of the supraoccipital bone (A-H) and the C1 vertebra (K-R) in control and *Myf5-Cre;Tgfbr2*$^{flox/flox}$ mice. C, D, G, H, M, N, Q, and R are enlarged from the boxes of A, B, E, F, K, L, O, and P, respectively.

(A, C) Muscle tissue forms continuous layers extending into the mid-dorsal region (black arrowheads) in control mice, and the dorsal tip of the perichondrium is expanding in the dorsal direction (black arrow). (B, D) Muscle tissue of conditional knockout mice does not extend into the mid-dorsal region (B, white arrowheads), and the perichondrium is disorganized at the dorsal tip (D, white arrow). (E-H) The primordium of the supraoccipital bone contains undifferentiated cartilage tissue in both control and conditional knockout mice. (I, J) *Type I collagen* (*Col I*) expression in control (I) and *Myf5-Cre;Tgfbr2*$^{flox/flox}$ (J) mice. *Col I* was expressed in the dorsal tip of the perichondrium (black arrow) in control

NIH-PA Author Manuscript

NIH-PA Author Manuscript

NIH-PA Author Manuscript

mice. *Col I* expression was compromised in the dorsal tip (white arrow) of conditional knockout mice. *Col I* expression was detectable surrounding the membrane of the supraoccipital bone primordium (black arrows). (K, M) The perichondrium from both sides of the neural arch is fused in the mid-dorsal region in control mice (black arrow). (L, N) The neural arch has detached in the dorsal area of the conditional knockout mice (white arrow). Muscle has attached to bone at the tip of the neural arch of C1 vertebra (white arrowhead). (O-R) Both control and conditional knockout mice have three zones, hypertrophic (h), proliferative (p), and resting (r). Scale bars: 200 μm in A-H and K-R, 100 μm in I-J.

NIH-PA Author Manuscript
NIH-PA Author Manuscript
NIH-PA Author Manuscript

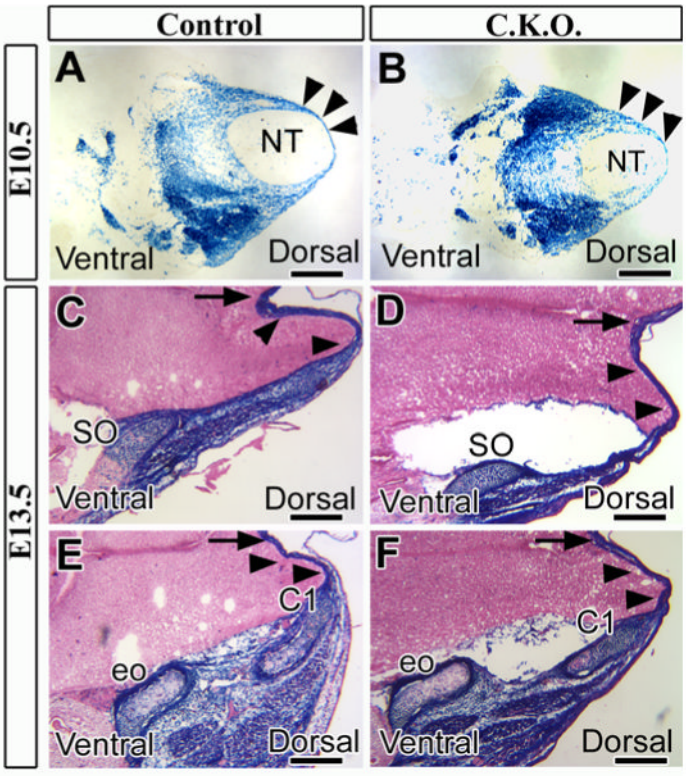

Figure 6. Cell migration from the dorsal sclerotome is unaffected in *Myf5-Cre;Tgfbr2*$^{flox/flox}$ mice

Cross sections stained for lacZ at E10.5 (A, B) and E13.5 (C-F). (A, B) Control (A: *Myf5-Cre;Tgfbr2*$^{flox/+}$*;R26R*$^{flox/+}$) and conditional knockout (B: *Myf5-Cre;Tgfbr2*$^{flox/flox}$*;R26R*$^{flox/+}$) mice contained mesoderm-derived cells (dark blue) migrating into the mid-dorsal area (black arrowheads). (C-F) Mesoderm-derived cells (black arrowheads) migrate to the mid-dorsal region in both control and conditional knockout mice, arriving at the supraoccipital bone (SO) and the neural arch of C1 vertebra (C1). Black arrows indicate the dorsal midline. Abbreviations: NT, neural tube; eo, exoccipital bone. Scale bars: 500 μm in A-F.

NIH-PA Author Manuscript
NIH-PA Author Manuscript
NIH-PA Author Manuscript

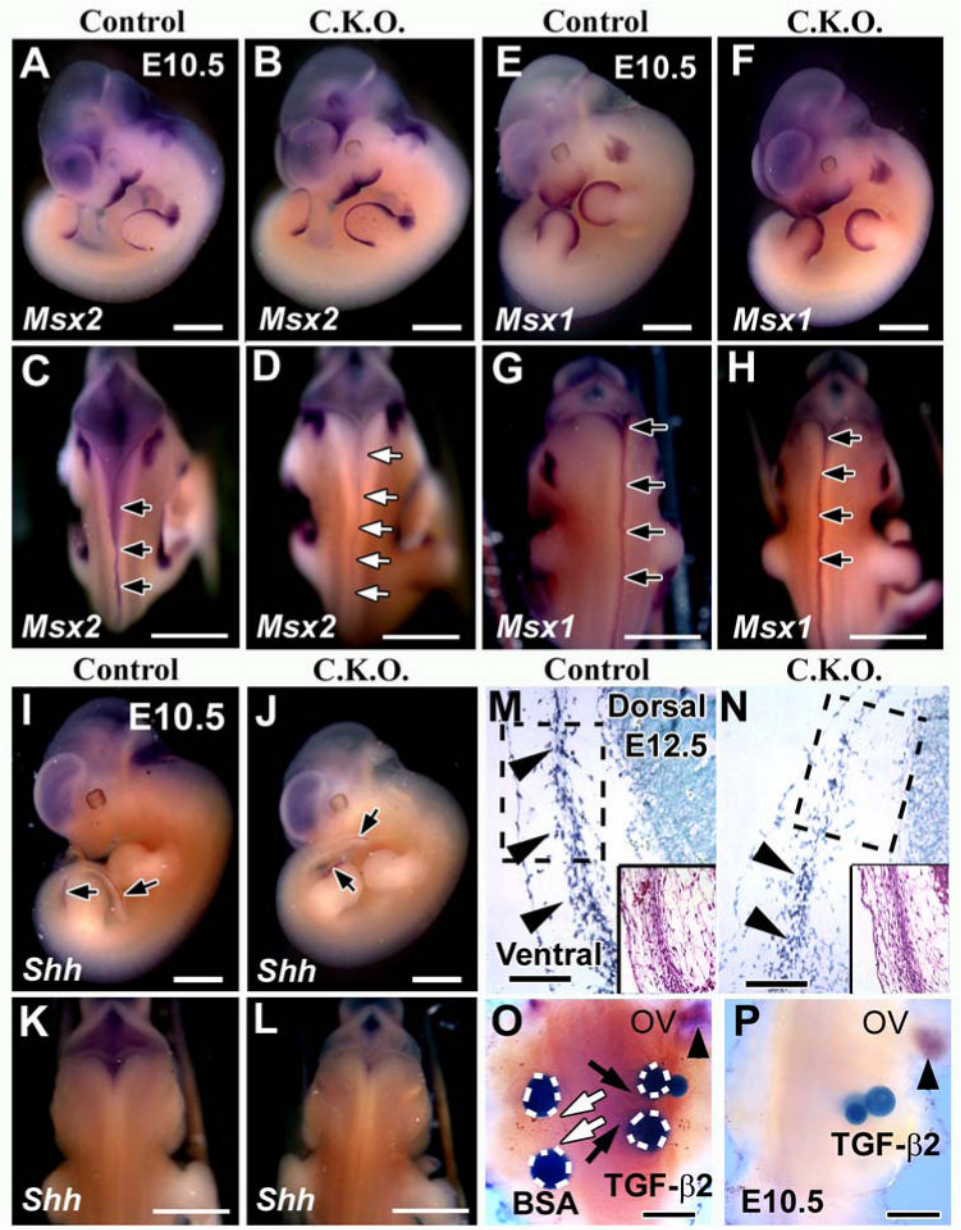

Figure 7. *Msx2* gene expression is altered in the mid-dorsal area of *Myf5-Cre;Tgfbr2*$^{flox/flox}$ mice

Msx2 (A-D), *Msx1* (E-H), and *Shh* (I-L) expression at E10.5 in control (A, C, E, G, I, K) and *Myf5-Cre;Tgfbr2*$^{flox/flox}$ mice (B, D, F, H, J, L). (A, B, E, F, I, J) lateral views. (C, D, G, H, K, L) dorsal views.

(A, B) *Msx2* expression is indistinguishable in lateral views of conditional knockout and control mice. (C, D) *Msx2* is expressed in the mid-dorsal region extending from rostral to caudal (black arrows) in control mice. *Msx2* expression is diminished in conditional knockout mice throughout the mid-dorsal region (white arrows). (E-H) *Msx1* expression in conditional knockout mice is indistinguishable from control in the mid-dorsal line extending from rostral to caudal (black arrows). (I-L) *Shh* expression in conditional knockout mice is indistinguishable from the control in the hind limb and tail bud (I, J, black arrows). *Shh* was negative at the dorsal area in both the control and the conditional knockout mice (K, L). (M, N) *Msx2* expression in mesenchyme cell cross sections at E12.5. Inserts show H.E. staining.

NIH-PA Author Manuscript

NIH-PA Author Manuscript

NIH-PA Author Manuscript

Msx2 expression is visible throughout the ventral region towards the dorsal region in the control mice (M, black arrowheads). *Msx2* expression is restricted to the ventral side of conditional knockout mice (N, black arrowheads). (O, P) Explants from the mid-dorsal area of E10.5 control and conditional knockout mice were treated with beads for 12 hours. The control sample (O) treated with TGF-β2 beads is positive for *Msx2* expression (black arrows, dark blue), but BSA beads do not induce *Msx2* expression (white arrows). The conditional knockout sample treated with TGF-β2 beads is negative for *Msx2* expression (P). *Msx2* gene expression is visible around the otic vesicle (ov) in both samples (black arrowhead). Scale bars: 1 mm in A-L, 100 μm in M, N, 200 μm in O, P.

NIH-PA Author Manuscript

NIH-PA Author Manuscript

NIH-PA Author Manuscript

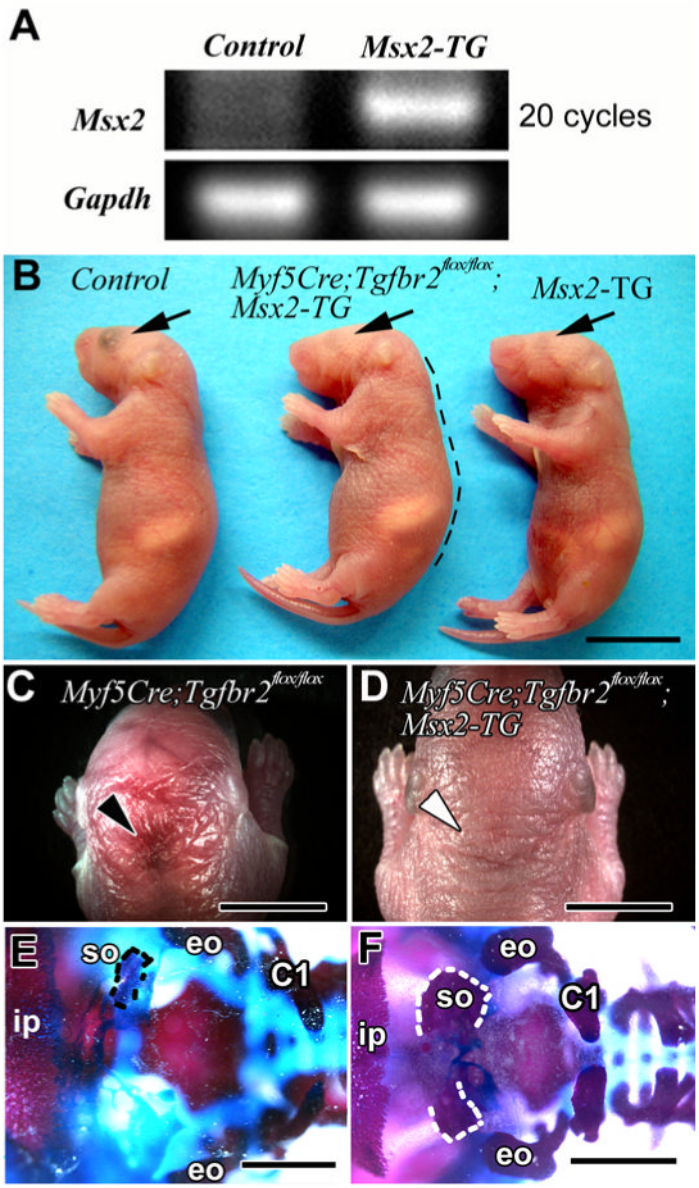

Figure 8. *Msx2* overexpression rescues the supraoccipital bone defect in *Myf5-Cre;Tgfbr2*$^{flox/flox}$ mice

(A) *Msx2* gene expression detected by PCR in control (*Tgfbr2*$^{flox/+}$) and *Msx2-TG* (*Msx2*$^{Tg/+}$;*Tgfbr2*$^{flox/+}$) samples at E10.5. (B) Whole mount views of *Myf5-Cre;Tgfbr2*$^{flox/+}$ (control), *Myf5-Cre;Tgfbr2*$^{flox/flox}$;*Msx2-TG* (transgenic) and *Msx2-TG* (transgenic) mice. The *Myf5-Cre;Tgfbr2*$^{flox/flox}$;*Msx2-TG* mouse has a hunchback phenotype like *Myf5-Cre;Tgfbr2*$^{flox/flox}$ mice (black dotted line) and microphthalmia like the *Msx2-TG* mouse (black arrows). (C) Dorsal view of the *Myf5-Cre;Tgfbr2*$^{flox/flox}$ mouse shows the hemorrhage around the occipital area (black arrowhead). (D) Dorsal view of the *Myf5-Cre;Tgfbr2*$^{flox/flox}$;*Msx2*-TG mouse shows no hemorrhage around the occipital area (white arrowhead). (E, F) Alizarin red and alcian blue staining. In a dorsal view, the *Myf5-Cre;Tgfbr2*$^{flox/flox}$ mouse has a diminished supraoccipital bone (E, black dotted line). The base of the supraoccipital bone is formed but each side is disconnected in the mid-dorsal area (F, white dotted line) in the *Myf5-Cre;Tgfbr2*$^{flox/flox}$;*Msx2-TG* mouse. Abbreviations:

C1, the neural arch of C1 vertebra; eo, exoccipital bone; ip, interparietal bone. Scale bars: 1 cm in B, 5 mm in C, D, 2 mm in E, F.

NIH-PA Author Manuscript
NIH-PA Author Manuscript
NIH-PA Author Manuscript

NIH-PA Author Manuscript
NIH-PA Author Manuscript
NIH-PA Author Manuscript

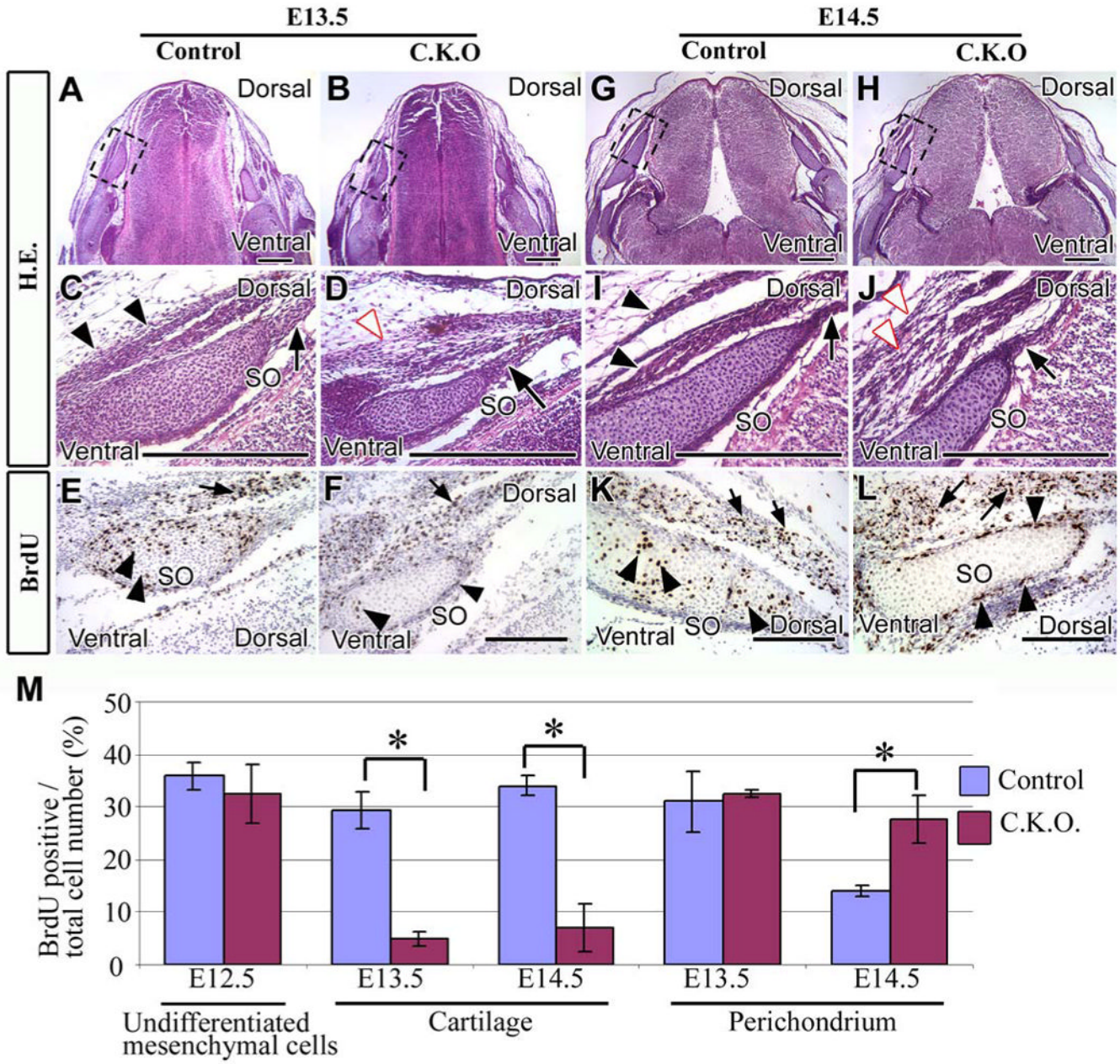

Figure 9. The pattern of cell proliferation is altered in the supraoccipital bone primordium of *Myf5-Cre;Tgfbr2*$^{flox/flox}$ mice

Cross sections of E13.5 (A-F) or E14.5 (G-L) supraoccipital bone primordium stained with hematoxylin and eosin (A-D, G-J) or BrdU (E, F, K, L). (C-F, I-L) Enlarged areas from the dashed black boxes of A, B, G, and H are shown in C/E, D/F, I/K, and J/L, respectively. (A, C) Control mice have well-organized perichondrium (C, black arrow) and muscle tissue (C, black arrowheads). (B, D) The perichondrium of conditional knockout mice is organized (D, black arrow), but muscle tissue is disorganized (D, white arrowhead). (E, F) Control and conditional knockout mice contain BrdU positive cells in the cartilage and the perichondrium of the supraoccipital bone (black arrowheads) and in the muscle cells (black arrow). (G, I) The perichondrium (I, black arrow) and muscle tissue (I, black arrowheads) are well-organized in control mice. (H, J) Conditional knockout mice have a well-organized

perichondrium (black arrow), but disorganized muscle tissue (J, white arrowheads). (K, L) In control mice, BrdU positive cells are present in both the cartilage and perichondrium of the supraoccipital bone (black arrowheads) and also in the muscle (black arrows). BrdU positive cells are visible in the muscle (black arrows) and perichondrium (black arrowheads) of the supraoccipital bone in conditional knockout mice, but not in the cartilage of supraoccipital bone. (M) Statistical analysis of cell proliferation activity in control and conditional knockout mice. Five randomly selected, non-overlapping samples were used to obtain the BrdU labeling index from each experimental group. Student t-tests were used for statistical analysis. *:$P<0.05$. Abbreviations: SO, the primordium supraoccipital bone. Scale bars: 300 μm in A-L.

NIH-PA Author Manuscript
NIH-PA Author Manuscript
NIH-PA Author Manuscript